Experimental studies of anode sheath phenomena in a Hall thruster discharge

L. Dorf,[a] Y. Raitses, and N. J. Fisch
Princeton Plasma Physics Laboratory (PPPL), Princeton, New Jersey 08543

(Received 19 October 2004; accepted 27 March 2005; published online 16 May 2005)

Both electron-repelling and electron-attracting anode sheaths in a Hall thruster were characterized by measuring the plasma potential with biased and emissive probes [L. Dorf, Y. Raitses, V. Semenov, and N. J. Fisch, Appl. Phys. Lett. **84**, 1070 (2004)]. In the present work, two-dimensional structures of the plasma potential, electron temperature, and plasma density in the near-anode region of a Hall thruster with clean and dielectrically coated anodes are identified. Possible mechanisms of anode sheath formation in a Hall thruster are analyzed. The path for current closure to the anode appears to be the determining factor in the anode sheath formation process. The main conclusion of this work is that the anode sheath formation in Hall thrusters differs essentially from that in the other gas discharge devices, such as a glow discharge or a hollow anode, because the Hall thruster utilizes long electron residence times to ionize rather than high neutral pressures.
 [DOI: 10.1063/1.1915516]

I. INTRODUCTION

In a gas discharge, there can be either an increase or a drop in the plasma potential over a distance of a few Debye lengths from the anode, generally referred to in the literature as the "anode fall" (Fig. 1). When the anode is at a higher potential than the near-anode plasma, the anode fall is called "positive," and when it is at a lower potential—"negative." The positive and negative anode falls are associated with the formation of the electron-attracting and electron-repelling anode sheaths, respectively. The anode sheath is a thin space-charge layer adjoint to the electrode. It is a nonlinear structure that was observed and studied by Langmuir and Mott–Smith in glow discharges.[1]

Anode sheath phenomena were studied comprehensively in other discharge devices such as a glow discharge,[2] which, as a Hall thruster (HT), is characterized by the discharge currents of no more than a few amperes, and a hollow-anode plasma source,[3–5] which, as a Hall thruster, is characterized by a relatively high degree of ionization, compared to that of the glow discharge. However, both glow discharge and hollow-anode plasma source typically operate at much higher neutral gas pressures (tens to hundreds of millitorrs versus few millitorrs in a HT); a hollow-anode plasma source is also characterized by much smaller discharge currents (tens of milliamperes versus amperes in a HT).

Experimental studies of the anode fall in glow discharges showed that at typical operating conditions the anode fall at a plane anode is positive.[2,6–9] At these conditions, the ion current flowing into a positive column is generated by ionization in a thin space-charge layer near the anode, with a voltage drop of the order of ionization potential of the working gas.[8–10] At higher discharge currents, of the order of several to ten amperes, the anode fall in the same discharge was observed to be negative[2] (note that at such high currents, a "glow discharge" is no longer an appropriate name for a low-pressure gas discharge). In this case, the thermal electron current to the anode, produced by ionization in the quasineutral plasma, is larger than the discharge current. Therefore, the formation of a negative fall is required to repel the excessive electron flux from the anode.[1,8] It was also observed experimentally for glow discharges that a decrease of the anode collecting surface area leads to altering of the anode fall from negative to positive.[2]

Furthermore, under certain conditions described later in this work, the near-anode region of a Hall thruster discharge can be compared to that of a hollow-anode plasma source.[3,4] A high degree of ionization inside the hollow-anode plasma source was attributed to the formation of a thick electron-attracting anode sheath, in which electrons gain kinetic energy of up to 40 eV.[5] Thus, the formation of a positive fall in a Hall thruster might be explained by the need for enhanced ionization; i.e., additional ionization in the sheath or inside the anode, which would increase the electron flux toward the anode collecting surface to the value determined by the discharge current. This and other possible mechanisms of anode fall formation require detailed investigation.

In spite of a number of experimental[11–22] and

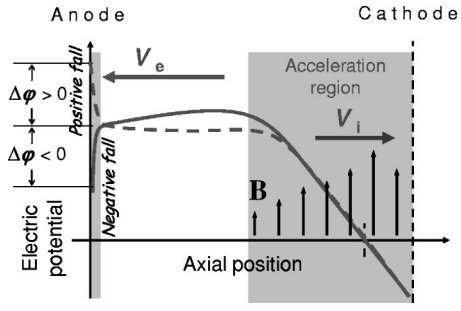

FIG. 1. Electric potential axial profile in Hall thrusters. The potential jump toward the anode, $\Delta\varphi > 0$, corresponds to the positive anode fall, and the potential drop, $\Delta\varphi < 0$, corresponds to the negative anode fall.

[a]Present address: Los Alamos National Laboratory, Los Alamos, NM 87545; electronic mail: ldorf@lanl.gov

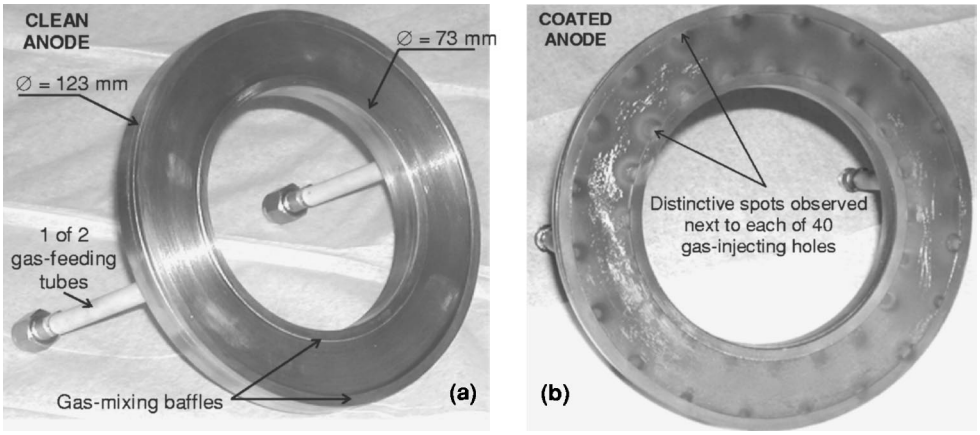

FIG. 2. Anode of the 2-kW Hall thruster (a) before and (b) after thruster operation. Accumulated lifetime >10 h.

theoretical[23–26] studies of a Hall thruster internal plasma structure, the understanding of the anode sheath phenomena in Hall thrusters was, until recently, very limited. A more detailed review of previous works and additional motivation for studying the anode sheath phenomena in Hall thrusters can be found in Refs. 27 and 28. As was reported recently, a diagnostic apparatus comprising biased and emissive electrostatic probes, a high-precision positioning system, and low-noise electronic circuitry was developed and used for measurements in the near-anode region of the 12.3-cm Hall thruster operating in the 0.2–2 kW power range.[27,29] Accurate, nondisturbing measurements of the plasma potential allowed the experimental identification of both electron-repelling (negative anode fall) and electron-attracting (positive anode fall) anode sheaths in a HT. Most interestingly, an intricate phenomenon revealed by the probe measurements is that the anode fall changes from positive to negative upon removal of the dielectric coating, which appears on the anode surface during the course of HT operation. The dependence of the sign and magnitude of the anode sheath on the discharge voltage and mass flow rate was also studied in Ref. 27, and the results of this investigation were found to be in agreement with our recent theoretical model.[27,28,30] Particularly, it was found that when the electron temperature, T_e, in the channel increases with the discharge voltage, V_d, the magnitude of the negative anode fall at a clean anode also increases with V_d.

In this paper, we again use the dielectric coating which appears on the anode surface as a natural way of decreasing the anode collecting surface area, and continue studying the anode sheath phenomena in the 2-kW Hall thruster for two different operating regimes—with clean and with coated anodes. A significant number of the biased probe measurements results only partially reported in Ref. 27 are presented in this work; the nature of the dielectric coating is identified; and, most importantly, possible mechanisms of anode sheath formation in a Hall thruster are analyzed.

The article is divided into five sections. In Sec. II, we report our most recent findings about the nature of the anode dielectric coating, and present pictures of the clean and coated anodes. In Sec. III, two-dimensional structures of the plasma potential, electron temperature, and plasma density in the near-anode region of a Hall thruster with clean and coated anodes are identified; also, the visual evidence of 2-kW Hall thruster operation in both cases is presented. In Sec. IV, possible mechanisms of anode sheath formation in a Hall thruster with clean and coated anodes are analyzed. We conclude in Sec. V with discussing possible practical implications of this work.

II. ANODE DIELECTRIC COATING

It was observed experimentally for the 2-kW Hall thruster in this study that a dielectric coating appears on the anode surface exposed to plasma after the thruster accumulates about ten or more hours of lifetime, operating at typical conditions (Fig. 2). A layer of coating was typically thin—about several tens of microns—and ranged in color from blue-green to golden-brown, with sometimes several colors present on the same coated anode. In some cases, after several tens of hours of thruster operation, the coating would accumulate to be up to 0.1 mm thick, and then it would split off—the scraps of coating were found at the bottom part of the channel. Furthermore, distinctive spots were observed next to each of the gas-injecting holes hidden under the gas-mixing baffles (Fig. 2).

To identify the chemical composition of the coating, three small samples were inserted under the baffle at the bottom part of the anode. Two samples were made out of the same material as the anode—stainless steel—and one sample was made out of tantalum. After several hours of thruster operation, the samples were extracted and a dielectric coating was observed on each of the samples. The coating on the tantalum sample was of a homogeneous blue-green color, and the coating on the stainless-steel samples was of a yellow-red color. The coatings on all three samples were then analyzed using energy dispersion spectroscopy (EDS). Results of EDS analysis—*counts per energy* spectra of the x-ray radiation emitted by the atoms of the coating as a result of electron bombardment—are given in Fig. 3. Interestingly, nitrogen is not present in any of the spectra (on the graphs, a potential nitrogen peak corresponds to the thin white line to the left of the oxygen peak). The presence of nitrogen in the coatings could be expected, as the thruster channel is made out of BN ceramic material. The carbon content cannot be

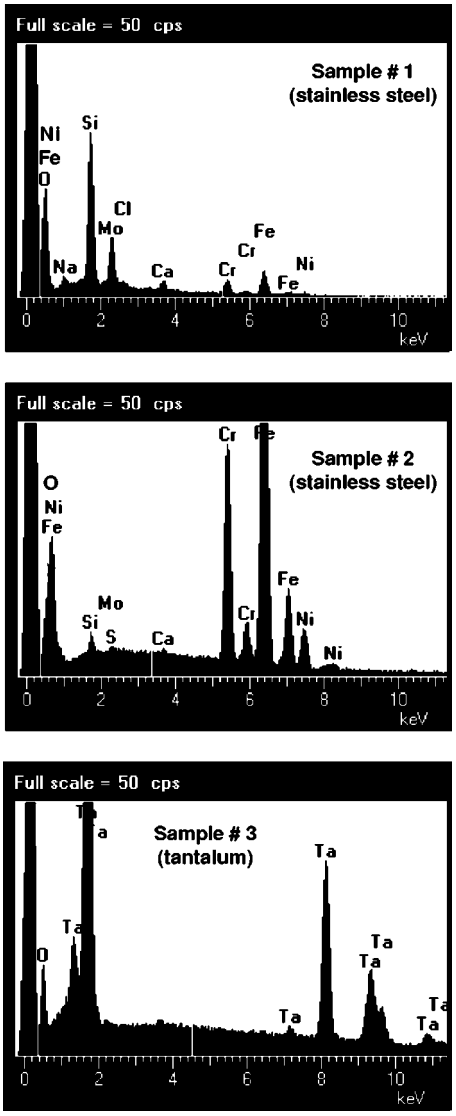

FIG. 3. Results of EDS analysis. A tall, wide peak at zero energy present on all three spectra is a reference mark added automatically by the software used in this analysis. The abscissa of each label with a name of a chemical element corresponds to the tabulated x-ray energy line for this element.

accurately quantified by the EDS analysis, because the corresponding x-ray energy is too low (on the graphs, the tabulated carbon energy line lies within the zero-energy peak). As can be seen from Fig. 3, a peak corresponding to the tabulated oxygen line is present on all three spectra, so it was ultimately decided that the coatings on all three samples are essentially the oxides of the substrate materials. The anode material, stainless steel, can indeed be expected to get oxidized during thruster operation, since the anode temperature could reach about 1000 °C at typical thruster operating conditions. A more detailed analysis of the EDS spectra and the description of the EDS technique can be found in Ref. 28.

It is still unclear, however, how oxygen gets into the thruster channel. Impurity limits data[28] for a research grade xenon used in the presented experiments suggest that only insignificant amount of oxygen enters the channel along with the xenon propellant, since the percentage of O_2 in the cylinder containing the supply of xenon is very low—less than 0.1 ppm. It can alternatively be suggested that the presence

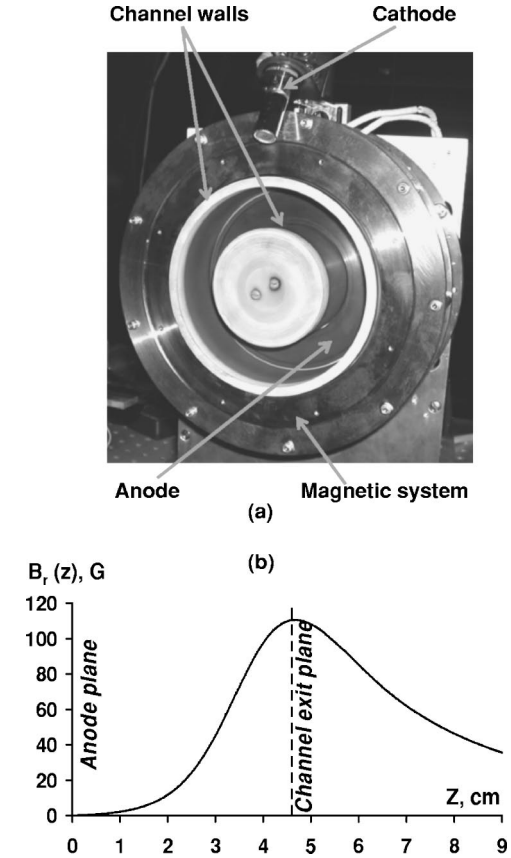

FIG. 4. (a) The 2-kW laboratory Hall thruster with 12.3-cm outer channel wall diameter. (b) Simulated radial magnetic-field axial profile, $B_r(z)$, used in the experiments. At $R=49$ mm—the midpoint between the channel walls.

of oxygen in the thruster channel is the vacuum facility effect—outgassing of the vacuum vessel walls, cryogenic pumps interior, and stainless-steel gas feed tubes could be one of the sources of oxygen, for example [note that the gas system was leak tested using Inficon UL200 helium leak detector, and the leak rate was observed to be no more than 10^{-8} mbar l/s $\approx 6\times10^{-7}$ SCCM (standard cubic centimeter per minute)]. A detailed investigation of oxygen origination and its content in the vacuum vessel needs to be conducted with the use of a residual gas analyzer (RGA) that is already installed on one of the ports of the Hall thruster experiment (HTX) vacuum vessel. Information about the content of oxygen in the background gas inside the vacuum vessel can then be used to estimate the anode surface oxidation rate and coating formation time.

III. NEAR-ANODE PLASMA STRUCTURE MEASUREMENTS

To investigate the effect of the anode collecting surface area on the anode sheath, the electrostatic probe apparatus described in Ref. 29 was employed for measurements in the near-anode region of the 2-kW Hall thruster with clean and coated anodes.[27] The thruster has a conventional annular configuration with a channel length of 4.6 cm [which is in the 2–8-cm range typical for HTs (Refs. 11–22)] and a channel width of 2.5 cm [Fig. 4(a)]. Typically, the thruster was operated at xenon gas mass flow rates of $\dot{m}=2-5$ mg/s, and

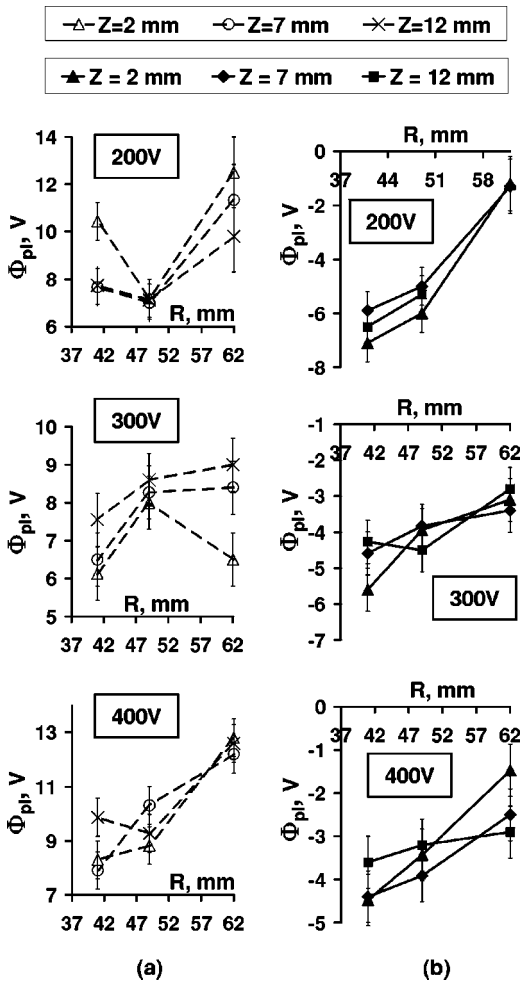

FIG. 5. Plasma potential radial profiles, $\Phi_{pl}(R)$, measured with the biased probe in the near-anode region of the 12.3-cm Hall thruster with (a) clean and (b) coated anodes at several distances from the anode, $Z=2-12$ mm, and several discharge voltages, $V_d=200-400$ V, for mass flow rate $\dot{m}=5$ mg/s. Zero potential is chosen at the anode.

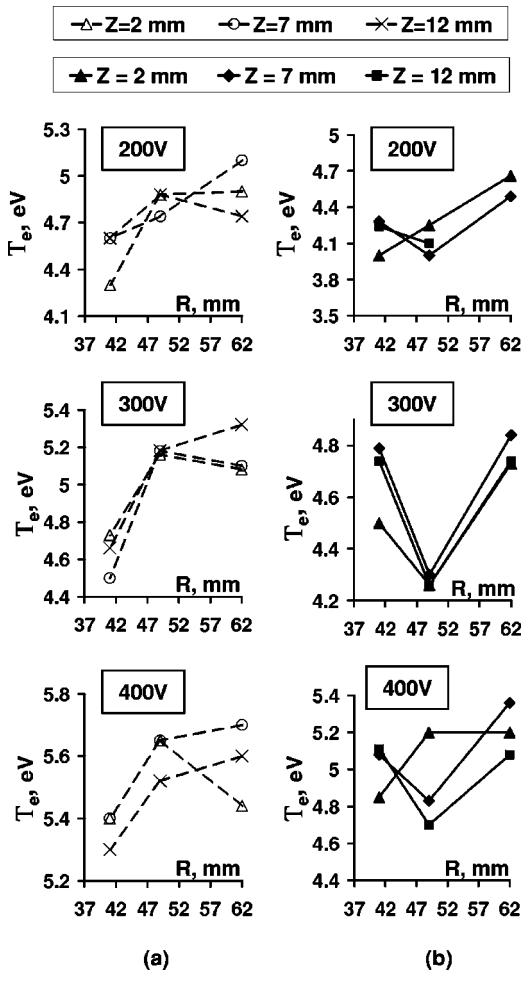

FIG. 6. Electron temperature radial profiles, $T_e(R)$, measured with the biased probe in the near-anode region of the 12.3-cm Hall thruster with (a) clean and (b) coated anodes at several distances from the anode, $Z=2-12$ mm, and several discharge voltages, $V_d=200-400$ V, for mass flow rate $\dot{m}=5$ mg/s.

in the discharge voltage range of $V_d=200-450$ V. In these experiments, the magnetic field was kept constant ($B\sim100$ G near the exit, at the midpoint between the channel walls). Figure 4(b) shows results of nonlinear simulations of the magnetic-field distribution. Simulations were conducted using a measured *B-H* curve of the low carbon steel used in the thruster design.

The plasma potential, plasma density, and electron temperature were measured at 2, 7, and 12 mm from the anode with the biased electrostatic probe. The probe was introduced radically into the near-anode region through the axial slot made in the outer channel wall. The plasma measurements were performed at several distances from the thruster axis: at the outer wall (OW), $R=62$ mm, in the midpoint between the channel walls (MC), $R=49$ mm, and at 4 mm from the inner wall (IW), $R=41$ mm. After the first set of experiments, the dielectric coating, which appears on the anode surface in the course of thruster operation, was removed, and a second set of experiments was conducted.

Figures 5(a), 6(a), 7(a), 5(b), 6(b), and 7(b) show the results of biased probe measurements in the near-anode region of the 2-kW Hall thruster with the clean and coated anodes, respectively, for $\dot{m}=5$ mg/s. Zero potential is chosen at the anode. The error bars shown in the plasma potential plots were computed using the error analysis described in Ref. 29. As can be seen from Fig. 5(a), in the case of the clean anode, the plasma potential at 2–12 mm from the anode is higher than the anode potential—the anode fall is negative. This indicates the presence of an electron-repelling anode sheath predicted theoretically in Hall thrusters.[23] Although there are many experimental studies of the HT plasma structure,[11,14–22] this appears to be the only reported experimental observation of the electron-repelling anode sheath in Hall thrusters up to date.

As can be seen from Fig. 5(b), in the case of the coated anode, the plasma potential at 2–12 mm from the anode is lower than the anode potential—the anode fall is positive. This indicates the presence of an electron-attracting anode sheath. Furthermore, it was observed that thruster operation with a coated anode is associated with a visual effect: the gas-injecting holes glow brighter than the bulk of the anode surface, with appearance of a jetlike structure from each hole [Fig. 8(b)]. When the anode front surface is coated with a dielectric, the discharge current supposedly closes to the an-

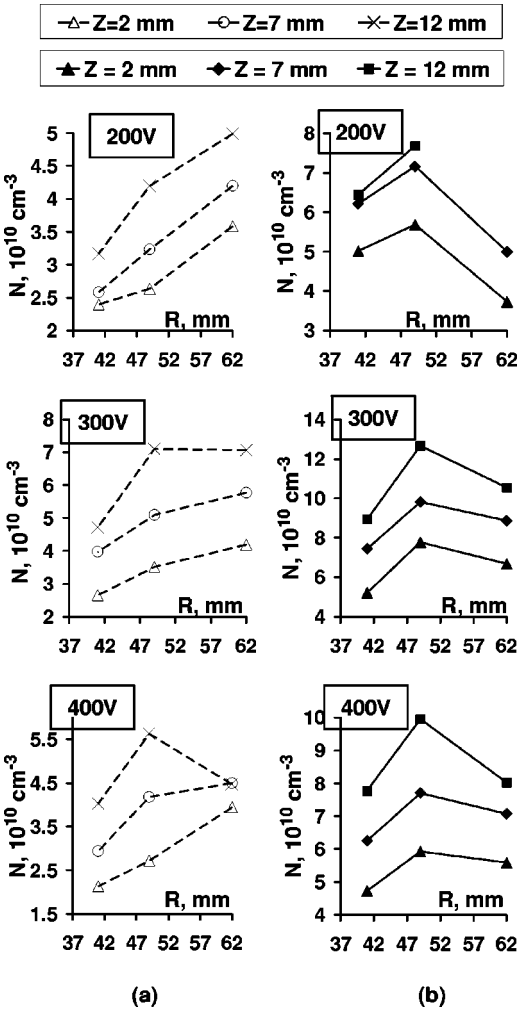

FIG. 7. Plasma density radial profiles, $N(R)$, measured with the biased probe in the near-anode region of the 12.3-cm Hall thruster with (a) clean and (b) coated anodes at several distances from the anode, $Z=2-12$ mm, and several discharge voltages, $V_d=200-400$ V, for mass flow rate $\dot{m}=5$ mg/s.

ode at the surfaces hidden under the baffles (Fig. 2), as these surfaces can remain conductive. Despite the fact that the plasma density measured near the coated anode is almost twice as large as that for the clean anode (Fig. 7), a total thermal current carried by the electrons entering the volume under the baffles is significantly smaller than the discharge current. An additional electron flux supposedly gets drawn in under the baffles by the electron-attracting sheath that appears at the inner, metal sides of the baffles. In Sec. IV, the above phenomena are discussed in greater detail.

Another interesting observation that can be readily made from Fig. 5 is that the plasma potential has a tendency to increase toward the outer channel wall for both clean and coated anodes. However, the electron (plasma) density has a tendency to decrease toward the outer wall in the case of the coated anode, and in the case of the clean anode, the radial structure of the electron density depends on the discharge voltage (Fig. 7). Assuming Boltzmann distribution for electrons in the near-anode plasma, where the magnetic field and the collision frequency are very small, one should expect the electron density to be higher where the plasma potential is higher. This discrepancy between the measured and expected behaviors of the plasma potential and electron density is not yet understood. It could be associated, for example, with a non-Maxwellian shape of the electron distribution function, which was observed in Hall thrusters.[31]

IV. POSSIBLE MECHANISMS OF ANODE FALL FORMATION

A. Neutral density distribution

To understand anode sheath formation, first it is useful to analyze the distribution of the neutral density near and inside the anode. For $\dot{m}=5$ mg/s, rough density estimations yield that mean free path for neutral-neutral collisions inside the anode and gas-injecting holes, $\Lambda_H \sim 0.1$ mm, is smaller than the diameter of the hole, $D_H=0.3$ mm (Fig. 9), so hydrodynamic Bernoulli equation for neutral pressure, P_n, neutral density, n_n, and neutral flow velocity, V_n, can be employed to relate flows inside the holes and inside the anode,

$$P_n + M_n n_n V_n^2/2 = \text{const}, \tag{1}$$

where $M_n=2.2\times10^{-22}$ g is the mass of a xenon atom.[32] Taking into account the flow continuity equation along with the fact that the cross-sectional area of the anode cavity (almost equal to the collecting surface area of the clean anode, $A_{\text{coll}}=77$ cm^2) is much larger than the combined cross-sectional area of the holes, $A_H=0.03$ cm^2, the dynamic pressure term can be neglected inside the anode. Similar to the problem of the flow of gas through the nozzle,[32] the neutral flow is assumed to have a sonic velocity inside the holes. For the

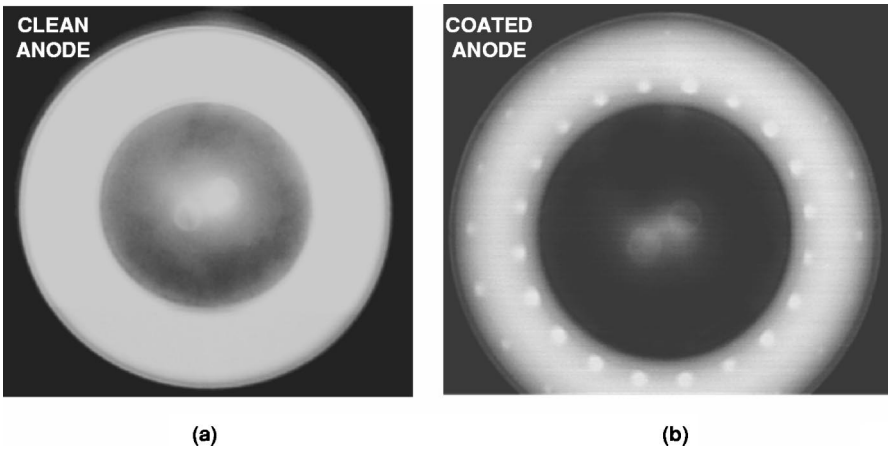

FIG. 8. Photographs of 12.3-cm Hall Thruster operation with (a) clean and (b) coated anodes. As can be seen, operation of the 12.3-cm HT with a coated anode is associated with a visual effect: the gas-injecting holes glow brighter than the bulk of the anode surface.

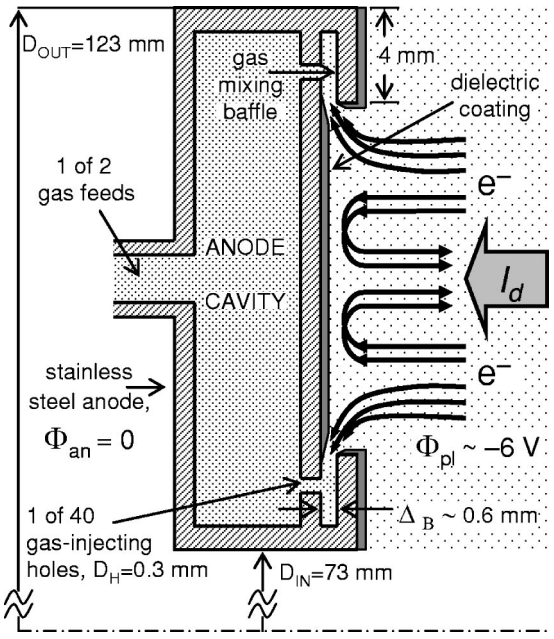

FIG. 9. Possible mechanism of the formation of a positive fall at the coated anode.

isothermal flow with the neutral temperature equal to the anode temperature, $T_A \approx 1000\ ^\circ\mathrm{C}$, using the anode dimensions given in Fig. 5, it can be finally estimated for $\dot{m} = 5$ mg/s that

(a) the neutral density inside the holes is

$$n_H = \dot{m}/(M_n A_H \sqrt{T_A/M_n}) = 2.7 \times 10^{16}\ \mathrm{cm}^{-3}, \tag{2}$$

(b) the static pressure in the holes is

$$P_H = n_H T_A \approx 3\ \mathrm{Torr}, \tag{3}$$

and it is twice as big as the dynamic pressure,

(c) the static pressure inside the anode is

$$P_A = 3/2 P_H \approx 4.5\ \mathrm{Torr}, \tag{4}$$

(d) the neutral density inside the anode is

$$n_A \approx 4 \times 10^{16}\ \mathrm{cm}^{-3}. \tag{5}$$

For the neutral-neutral collision cross-section $\sigma_{nn} \approx 3 \times 10^{-15}\ \mathrm{cm}^2$, the length of the mean free path inside the holes can be estimated as

$$\Lambda_H = 1/(\sigma_{nn} n_H) \approx 0.12\ \mathrm{mm}, \tag{6}$$

which is smaller than the hole diameter, $D_H = 0.3$ mm. This estimation supports the aforementioned assumption of the hydrodynamic flow inside the holes. Assume now that after the jets that are coming out of the gas-injecting holes hit the baffles (Fig. 9), the neutral gas spreads out and homogeneously fills up the volume under the baffles. Then, assuming that the neutral gas leaves the volume under the baffles and enters the channel with the velocity of a free atomic flow, $V_a = \sqrt{T_A/(2\pi M_n)} \approx 113$ m/s, the average neutral density, neutral pressure, and the length of the mean free path for neutral-neutral collisions under the baffles can be estimated as

$$n_B \approx \dot{m}/(M_n V_a A_B) \approx 5.5 \times 10^{14}\ \mathrm{cm}^{-3}, \tag{7}$$

$$P_B = n_B T_A \approx 75\ \mathrm{mTorr}, \tag{8}$$

$$\Lambda_B = 1/(\sigma_{nn} n_B) \approx 6\ \mathrm{mm}, \tag{9}$$

respectively. In the above estimation, $A_B = \pi(D_{\mathrm{out}} + D_{\mathrm{in}})\Delta_B \approx 3.7\ \mathrm{cm}^2$ is the area of the surface through which the gas leaves the volume under the baffles, calculated using the dimensions given in Fig. 9. Finally, when the neutral gas distributes uniformly[33] over the entire channel cross section and bleeds through the channel with the velocity V_a, the density, pressure, and the length of the mean free path near the anode can be estimated as

$$n_C \approx \dot{m}/(M_n V_a A_{\mathrm{coll}}) \approx 2.6 \times 10^{13}\ \mathrm{cm}^{-3}, \tag{10}$$

$$P_C = n_C T_A \approx 3.5\ \mathrm{mTorr}, \tag{11}$$

$$\Lambda_C = 1/(\sigma_{nn} n_C) \approx 12\ \mathrm{cm}, \tag{12}$$

respectively.

B. Formation of a negative fall at the clean anode

In the quasineutral plasma between the clean anode and the acceleration region, the electron drift velocity,

$$V_{\mathrm{dr}} \sim I_d/(enA_{\mathrm{ch}}) \approx 10^7\ \mathrm{cm/s}, \tag{13}$$

is much smaller than the average velocity of the half-Maxwellian electron flux that would be traveling toward the anode in the absence of an electron-repelling anode sheath,

$$V_{\mathrm{HM}} = \sqrt{2T_e/(\pi m_e)} \approx 8 \times 10^7\ \mathrm{cm/s}. \tag{14}$$

The above estimations were made using the channel cross-section $A_{\mathrm{ch}} = A_{\mathrm{coll}} = 77\ \mathrm{cm}^2$, the measured discharged current, $I_d = 4.35$ A, and the plasma density, n, along with the electron temperature, T_e, measured in the midpoint between the channel walls at 2 mm from the anode for $V_d = 200$ V and $\dot{m} = 5$ mg/s [Figs. 6(a) and 7(a)]. Thus, the thermal electron flux to the anode would carry an electric current much greater than the discharge current. At mass flow rates typical for the 2-kW Hall thruster, electron-neutral collisions are very weak near the anode ($\Lambda_{\mathrm{en}} \sim \Lambda_{\mathrm{nn}} \approx 12$ cm), so is the magnetic field in the conventional configuration.[28] Therefore, formation of an electron-repelling anode sheath (negative anode fall) is required to repel an excessive electron flux from the anode. A reversed electron flux created in the electron-repelling anode sheath decreases the net electron velocity in the quasineutral plasma near the anode to the value V_{dr} determined by the discharge current, thus providing current continuity everywhere.

C. Formation of a positive fall at the coated anode

In the case of the coated anode (Fig. 9), the electron drift velocity in the quasineutral plasma between the coated anode and the acceleration region is even smaller,

$$V_{\mathrm{dr}} \sim I_d/(enA_{\mathrm{ch}}) \approx 5 \times 10^6 \text{ cm/s}. \quad (15)$$

That is because for the same operating conditions, the plasma density measured near the coated anode is almost twice as big as it is near the clean anode (Fig. 7), while the discharge currents are similar, and the channel cross section is the same. Since the electron thermal velocity is almost the same as in the case of the clean anode (Fig. 6), formation of an *electron-repelling sheath* at the *coated anode surface* is again required to decrease the net electron velocity in the quasineutral plasma near the anode from V_{HM} to V_{dr}. By reflecting electrons and creating an ion backflow this sheath also allows satisfying the condition of a zero net current to a dielectric.

While the anode surface exposed to plasma gets coated with a dielectric, some elements of the anode surface, for example, the inner side of the gas-mixing baffles or the interior of the gas-injecting holes and the anode cavity, may remain conductive (Fig. 9). When the anode front surface is coated with a dielectric, the discharge current should close to the anode at these conductive surfaces by the electrons that are not repelled. Understanding the path and mechanism of the current closure to the anode could therefore reveal the physics of the anode fall formation process. We shall now analyze the feasibility of three possible mechanisms of the current closure to the anode and anode fall formation.

1. Electron-attracting anode sheath

Consider that the discharge current closes to the anode at the inner, metal side of the gas-mixing baffles. A half-Maxwellian electron flux entering the volume under the baffles (Fig. 9) carries the electric current

$$I_{\mathrm{HM}} = 1/2(1.5n)\sqrt{2T_e/(\pi m_e)}eA_B \approx 1.76 \text{ A}, \quad (16)$$

which constitutes about 40% of the measured discharge current, $I_d = 4.32$ A. The above estimation was made using the plasma density, n, and electron temperature, T_e, measured in the midpoint between the channel walls at 2 mm from the anode for $V_d = 200$ V and $\dot{m} = 5$ mg/s [Figs. 6(b) and 7(b)], and considering the maximum ($\sim 50\%$) relative error in determining the plasma density from biased probe measurements.[29] The remainder 60% of the electron flux supposedly gets drawn in under the baffles by the *electron-attracting sheath* that appears at the inner, *metal sides* of the baffles. Due to this sheath, the near-anode plasma potential appears to be about 4–6 V lower than the anode potential [Fig. 5(b)]. The plasma in this electron-attracting sheath can be almost purely electron, like in a vacuum diode, since its characteristic scale, $\Delta_B = 0.6$ mm (Fig. 9), is only several Debye lengths estimated at 2 mm from the anode,

$$\lambda_D = \sqrt{T_e/(4\pi n_e e^2)} \sim 0.075 \text{ mm}. \quad (17)$$

The electron density under the baffles in the case of the coated anode is much larger than in the case of the clean anode, in which only the electrons that penetrate through the electron-repelling sheath enter the volume under the baffles. This could explain such intricate phenomena as distinctive glowing next to each of the gas-injecting holes (where the neutral density is the largest) observed during operation of the 12.3-cm Hall thruster with the coated anode [Fig. 8(b)].

2. Filamentation

Note that the anode design shown in Fig. 2 is specific to the 12.3-cm Hall thruster in this study; in general, anode may be constructed without gas-mixing baffles,[33] or even be separated from a gas distributor.[15,34] Interestingly, operation of a Hall thruster with the coated anode was also observed in the case when the anode design does not include gas-mixing baffles and when there are no gaps between the anode and the channel walls.[35] In this case, the discharge current should close to the anode at the interior of the gas-injecting holes or at the inner side of the anode cavity. To achieve the measured discharge current, the electron density inside the holes needs to be

$$n_{eH} \sim I_d/(eA_H V_{eH}) \approx 7 \times 10^{12} \text{ cm}^{-3}, \quad (18)$$

where $V_{eH} \approx 1.3 \times 10^8$ cm/s is the velocity of the monoenergetic electron flux accelerated in the potential difference between the anode, $\Phi = 0$, and the plasma, $\Phi = \Phi_{\mathrm{pl}} \sim -(4-6)$ V, to the energy

$$E_{eH} = T_e - e\Phi_{\mathrm{pl}} \sim 10 \text{ eV}. \quad (19)$$

The above estimation is made assuming that Φ_{pl} in the aforementioned work was of the same order as Φ_{pl} in this study. The characteristic voltage drop associated with such electron density,

$$\Delta\Phi \sim en_{eH}D_H^2 \approx 1.2 \text{ kV}, \quad (20)$$

is much larger than the plasma potential measured relative to the anode. Therefore, plasma needs to be quasineutral inside the holes, with anode fall supposedly concentrated at the walls of the holes or at the inner anode surface. The mechanism that could be responsible for the formation of such ultrahigh-density plasma channels in front of each hole is not yet understood.

3. Enhanced ionization

It was observed experimentally for Hall thrusters that penetration of the electrons into the anode cavity can cause ionization of the neutral gas inside the anode.[12] Furthermore, near the anode, the discharge of a Hall thruster with a coated anode can be compared to that of a relatively well-studied hollow-anode plasma source,[3,4] as the coated anode has two essential features of the hollow anode: a collecting surface area that is significantly smaller than the cross-sectional area of the discharge chamber, and an insulated front surface. A high degree of ionization inside the hollow-anode plasma source—near-anode electron density of 10^{10}–10^{11} cm^{-3} at nitrogen flow rate of 25 SCCM—was attributed to the formation of a thick electron-attracting anode sheath, in which electrons gain kinetic energy of up to 40 eV.[5] Thus, it can be suggested that the formation of a positive fall at the coated anode in the 2-kW Hall thruster could be explained by the need for enhanced ionization: additional ionization in the sheath or inside the anode would increase the electron flux toward anode conductive surfaces to the value determined by the discharge current.[27] However, the neutral gas pressure in

front of the anode in a hollow-anode plasma source is about 100 times larger (and therefore the ionization length is about 100 times smaller) than it is near the coated anode in a Hall thruster.[5] Furthermore, as it was later reported by Melikov in Ref. 13, noticeable ionization inside the anode occurs only if the anode temperature is lower than $\sim 500\,^{\circ}\mathrm{C}$. At higher temperatures, the neutral pressure, $p_n \geqslant 2$ Torr, becomes comparable to the electron pressure, $p_e \sim 1.9$ Torr, and the discharge is carried by the gas flow out of the anode cavity (these estimations were made for the plasma density $n = 10^{10}\ \mathrm{cm}^{-3}$, electron temperature $T_e = 8$ eV, and mass flow rate of 2 mg/s).

The following estimations can be used to demonstrate that the formation of a positive anode fall at the coated anode in the 2-kW Hall thruster is unlikely to be explained by the need for enhanced ionization. For a half-Maxwellian electron flux with the temperature $T_{eB} \sim 10$ eV and neutral densities calculated in Sec. IV A, ionization lengths in front of the anode, under the baffles, inside the gas-injecting holes, and inside the anode can be estimated as

$$\Lambda_C^i \sim 1/(\langle \sigma^i \rangle n_C) \approx 1\ \mathrm{m}, \tag{21}$$

$$\Lambda_B^i \sim 4.5\ \mathrm{cm}, \tag{22}$$

$$\Lambda_H^i \sim 1\ \mathrm{mm}, \tag{23}$$

$$\Lambda_A^i \sim 0.6\ \mathrm{mm}, \tag{24}$$

respectively. Here,

$$\langle \sigma^i \rangle = \langle \sigma^i V_e \rangle / V_{\mathrm{HM}} \approx 4 \times 10^{-16}\ \mathrm{cm}^2 \tag{25}$$

is the energy-dependent electron-impact ionization cross section for xenon atoms, averaged over the half-Maxwellian distribution.[28,36] Thus, significant multiplication of the electron flux entering the volume under the baffles could occur only inside the holes or inside the anode. While electrons produced by ionization would reach the metal surface and contribute to the discharge current, corresponding ions would have to stream out into the channel and recombine with electrons at the anode dielectric surface, to provide charge conservation and current continuity everywhere. As follows from the estimations above, the ion flux from the volume under the baffles would then represent about 60% of the discharge current, so the ion density under the baffles can be estimated as

$$n_{iB} \sim 0.6 I_d / (e V_{iB} A_B) \approx 3.3 \times 10^{13}\ \mathrm{cm}^{-3}, \tag{26}$$

assuming ions are accelerated in the positive anode fall to the velocity

$$V_{iB} \sim \sqrt{e \Phi_{\mathrm{pl}} / M_{\mathrm{Xe}}} \approx 2 \times 10^5\ \mathrm{cm/s}. \tag{27}$$

As in Sec. IV C 2, we expect here that the positive anode fall (electron-attracting anode sheath) is concentrated at the walls of the holes or at the inner anode surface. If we assume that ions stream out of the anode cavity through the gas-injecting holes, the plasma density inside the holes in this case would have to be even larger than that given by Eq. (26), since $A_B/A_H \sim 100$. However, the plasma densities measured inside the Hall thruster anode,[12] in the vicinity of the anode hole in a hollow-anode plasma source,[5] and at 2 mm from the anode in the 12.3-cm Hall thruster (Fig. 7) were observed to be of the order of $10^{10} - 10^{11}\ \mathrm{cm}^{-3}$. Thus, additional ionization inside the anode and gas-injecting holes is unlikely to be the process that maintains current balance at the anode surface, from which we conclude that the formation of a positive fall at the coated anode is unlikely to be explained by the need for enhanced ionization.

V. SUMMARY AND DISCUSSION

Probe measurements showed that the anode sheath in Hall thrusters can be electron repelling or electron attracting, depending on the anode collecting surface area, namely, the anode fall changes from positive to negative upon removal of the dielectric coating, which appears on the anode surface during the normal course of Hall thruster operation. When the anode front surface is coated with a dielectric, the discharge current should close to the anode at the surfaces that remain conductive. However, a total thermal electron current toward the conductive area is significantly smaller than the discharge current. In this paper, we have analyzed the feasibility of three possible mechanisms of the current closure to the anode and anode fall formation:

(1) an additional electron flux is attracted toward the conductive surfaces—the inner side of the gas-mixing baffles—by the electron-attracting sheath that appears at these surfaces,
(2) the discharge current closes to the anode at the interior of the gas-injecting holes or at the inner side of the anode cavity—and that is where the positive anode fall (electron-attracting anode sheath) is concentrated—via the formation of the ultrahigh-density electron current channels in front of each hole, and
(3) the discharge current closes to the anode at the same surfaces as in (2), but via additional ionization inside the anode and/or gas-injecting holes.

Our analysis indicates the pitfalls of the mechanisms (2) and (3) above, thus leaving us with (1) as the preferred mechanism. The main conclusion of this paper is that the anode sheath formation in Hall thrusters differs essentially from that in the other gas discharge devices, such as a glow discharge or a hollow anode, because the Hall thruster utilizes long electron residence times to ionize rather than high neutral pressures.

Note that understanding the anode sheath structure in the case of a coated anode might be useful for designing a thruster anode. It is yet unclear how oxygen that forms the anode dielectric coating (oxide layer) gets into the discharge chamber, but since the vacuum facility used in the presented experiments is typical for studies of a Hall thruster, it can be suggested that the coating formation is a general issue for laboratory Hall thrusters.[37] Moreover, if oxygen enters the thruster channel along with the xenon propellant, this issue could also be expected for thrusters used in actual space applications. Therefore, when designing an anode (which is not necessarily also a gas distributor) for a HT, one has to ensure that some surfaces will remain conductive if the an-

ode front surface gets coated with a dielectric, so that the combined conductive surface area is sufficient for passing a discharge current. Furthermore, the electron energy flux toward these surfaces in the case of a coated anode will be much higher than in the case of a clean anode, in which only the electrons that penetrate through the electron-repelling sheath reach the anode; plus, electrons gain additional kinetic energy while moving inside the electron-attracting sheath toward the anode conductive surfaces. At $V_d = 200$ V and $\dot{m} = 5$ mg/s, the power per unit area, deposited at the conductive surfaces of the clean and coated anodes, can be estimated as

$$P_{\text{clean}} \sim (I_d/A_{\text{coll}})(2T_e/e + |\Delta\varphi_{\text{sh}}|) \sim 1 \text{ W/cm}^2, \tag{28}$$

$$P_{\text{coated}} \sim (I_d/A_B)(2T_e/e + |\Delta\varphi_{\text{sh}}|) \sim 17 \text{ W/cm}^2, \tag{29}$$

respectively (effect of the secondary electron emission was neglected in this calculation, since the characteristic electron energy at the anode, $E \sim 2T_e + e|\Delta\varphi_{\text{sh}}|$, does not exceed 25 eV for both anodes). Thus, one also has to ensure that conductive surfaces of the coated anode will not overheat during thruster operation.

Finally, note that the anode dielectric coating might have a positive effect on Hall thruster operation. As was reported in Refs. 27 and 28, high-amplitude discharge current oscillations in the 1–100-kHz wave band, which are inherent to Hall thrusters,[38] are attenuated by up to a factor of two, when the anode of the 12.3-cm Hall thruster is coated with dielectric. Therefore, it may be suggested that significant mitigation of the oscillations with respect to the initial level, observed in several extensive life tests,[39–43] is associated with the formation of the anode dielectric coating.[28]

ACKNOWLEDGMENTS

The authors are very grateful to Artem Smirnov for his help with analyzing the possible mechanisms of anode fall formation. They would also like to thank Dr. Vladimir Semenov and David Staack for fruitful discussions. The EDS analysis of the anode dielectric coating was performed by Stork MMA Testing Laboratories (Newtown, PA). This work was supported by US DOE Contract No. AC02-76CH0-3073 and NJ Commission for Science and Technology.

[1] I. Langmuir and H. M. Mott-Smith, Gen. Electr. Rev. **27**, 449 (1924); see also *The Collected Works of Irving Langmuir*, edited by C. G. Suits and H. E. Way (Pergamon, New York, 1961), Vol. 4.
[2] B. N. Kliarfeld and N. A. Neretina, Sov. Phys. Tech. Phys. **3**, 271 (1958).
[3] V. I. Miljevic, Rev. Sci. Instrum. **55**, 931 (1984).
[4] V. I. Miljevic, Appl. Opt. **23**, 1598 (1984).
[5] A. Anders and S. Anders, Plasma Sources Sci. Technol. **4**, 571 (1995).
[6] G. Francis, in *Encyclopedia of Physics*, Handbuch der Physik, Vd. XXII edited by S. Flugge (Springer, Berlin, 1956), pp. 53–208.
[7] A. von Engel, *Ionized Gases* (Clarendon, Oxford, 1965), Sec. 8.1.
[8] V. L. Granovsky, *Electric Current in Gas. Steady Current* (Nauka, Moscow, 1971), Sec. 58 (in Russian).
[9] Yu. P. Raizer, *Gas Discharge Physics* (Springer, Berlin, 1997), Sec. 8.10.
[10] L. D. Tsendin, Zh. Tekh. Fiz. **56**, 278 (1986).
[11] A. I. Morozov, Yu. V. Esinchuk, G. N. Tilinin, A. V. Trofimov, Yu. A. Sharov, and G. Ya. Shchepkin, Sov. Phys. Tech. Phys. **17**, 38 (1972).
[12] I. V. Melikov, Sov. Phys. Tech. Phys. **19**, 35 (1974).
[13] I. V. Melikov, Sov. Phys. Tech. Phys. **22**, 452 (1977).
[14] A. M. Bishaev and V. Kim, Sov. Phys. Tech. Phys. **23**, 1055 (1978).
[15] G. Guerrini, C. Michaut, M. Dudeck, A. N. Vesselovzorov, and M. Bacal, *Proceedings of the 25th International Electric Propulsion Conference*, Cleveland, OH, August 1997 (Electric Rocket Propulsion Society, Cleveland, OH, 1997), IEPC Paper 1997-053.
[16] Y. Raitses, J. Ashkenazy, and M. Guelman, J. Propul. Power **14**, 247 (1998).
[17] Y. Raitses, L. A. Dorf, A. A. Litvak, and N. J. Fisch, J. Appl. Phys. **88**, 1263 (2000).
[18] N. J. Fisch, Y. Raitses, L. A. Dorf, and A. A. Litvak, J. Appl. Phys. **89**, 2040 (2001).
[19] Y. Raitses, M. Keidar, D. Staack, and N. J. Fisch, J. Appl. Phys. **92**, 4906 (2002).
[20] J. M. Haas and A. D. Gallimore, Phys. Plasmas **8**, 652 (2001).
[21] N. B. Meezan, W. A. Hargus, Jr., and M. A. Cappelli, Phys. Rev. E **63**, 026410 (2001).
[22] N. Z. Warner, J. J. Szabo, and M. Martinez-Sanchez, *Proceedings of the 28th International Electric Propulsion Conference*, Toulouse, France, March 2003 (Electric Rocket Propulsion Society, Cleveland, OH, 2003), IEPC Paper 2003-082.
[23] E. Ahedo, P. Martinez-Cerezo, and M. Martinez-Sanchez, Phys. Plasmas **8**, 3058 (2001).
[24] A. Fruchtman, N. J. Fisch, and Y. Raitses, Phys. Plasmas **8**, 1048 (2001).
[25] M. Keidar, I. Boyd, and I. Beilis, *Proceedings of the 38th Joint Propulsion Conference and Exhibit*, Indianapolis, IN, July 2002 (American Institute of Aeronautics and Astronautics, Reston, VA, 2002), AIAA Paper 2002-4107.
[26] L. Dorf, V. Semenov, Y. Raitses, and N. J. Fisch, *Proceedings of the 38th Joint Propulsion Conference and Exhibit*, Indianapolis, IN, July 2002 (American Institute of Aeronautics and Astronautics, Reston, VA, 2002), AIAA Paper 2002-4246.
[27] L. Dorf, Y. Raitses, V. Semenov, and N. J. Fisch, Appl. Phys. Lett. **84**, 1070 (2004).
[28] L. Dorf, Ph.D. dissertation, Princeton University, 2004.
[29] L. Dorf, Y. Raitses, and N. J. Fisch, Rev. Sci. Instrum. **75**, 1255 (2004).
[30] L. Dorf, V. Semenov, and Y. Raitses, Appl. Phys. Lett. **83**, 2551 (2003).
[31] A. I. Bugrova, L. M. Volkova, V. A. Ermolenko, E. A. Kral'kina, A. M. Devyatov, and V. K. Kharchevnikov, High Temp. **19**, 822 (1981).
[32] L. D. Landau and E. M. Lifshitz, in *Course of Theoretical Physics*, 2nd ed. (Butterworth-Heinemann, Oxford, 1987), Vol. 6.
[33] V. Vial, A. Lazurenko, C. Laure, and A. Bouchoule, *Proceedings of the 28th International Electric Propulsion Conference*, Toulouse, France, March 2003 (Electric Rocket Propulsion Society, Cleveland, OH, 2003), IEPC Paper 2003-0221.
[34] A. I. Morozov and V. V. Savelyev, in *Reviews of Plasma Physics*, edited by B. B. Kadomtsev and V. D. Shafranov (Kluwer Academic, New York, 2000), Vol. 21, p. 386.
[35] Y. Raitses (unpublished).
[36] D. Rapp and P. Englander-Golden, J. Chem. Phys. **43**, 1464 (1965).
[37] A. I. Morozov and V. V. Savelyev, in *Reviews of Plasma Physics*, edited by B. B. Kadomtsev and V. D. Shafranov (Kluwer Academic, New York, 2000), Vol. 21, pp. 214 and 377.
[38] E. Y. Choueiri, Phys. Plasmas **8**, 1411 (2001).
[39] C. E. Garner, J. E. Polk, K. D. Goodfellow, and J. R. Brophy, *Proceedings of the 23rd International Electric Propulsion Conference*, Seattle, WA, September 1993 (Electric Rocket Propulsion Society, Cleveland, OH, 1993), IEPC Paper 1993-091.
[40] C. E. Garner, J. R. Brophy, J. E. Polk, and L. C. Pless, *Proceedings of the 30th Joint Propulsion Conference and Exhibit*, Indianapolis, IN, June 1994 (American Institute of Aeronautics and Astronautics, Reston, VA, 1994), AIAA Paper 1994-2856.
[41] T. Randolph, G. Fischer, J. Kahn, H. Kaufman, V. Zhurin, K. Kozubsky, and V. Kim, *Proceedings of the 30th Joint Propulsion Conference and Exhibit*, Indianapolis, IN, June 1994 (American Institute of Aeronautics and Astronautics, Reston, VA, 1994), AIAA Paper 1994-2857.
[42] V. Kim, J. Brophy, M. Day, C. Garner, T. Randolph, and A. Sorokin, *Proceedings of the 31st Joint Propulsion Conference and Exhibit*, San Diego, CA, July 1995 (American Institute of Aeronautics and Astronautics, Reston, VA, 1995), AIAA Paper 1995-2669.
[43] B. A. Arhipov, A. S. Bober, R. Y. Gnizdor, K. N. Kozubsky, A. I. Korakin, N. A. Maslennikov, and S. Y. Pridannikov, *Proceedings of the 24th International Electric Propulsion Conference*, Moscow, Russia, September 1995 (Electric Rocket Propulsion Society, Cleveland, OH, 1995), IEPC Paper 1995-039.